

## **Distribution Agreement**

In presenting this thesis as a partial fulfillment of the requirements for a degree from Emory University, I hereby grant to Emory University and its agents the non-exclusive license to archive, make accessible, and display my thesis in whole or in part in all forms of media, now or hereafter now, including display on the World Wide Web. I understand that I may select some access restrictions as part of the online submission of this thesis. I retain all ownership rights to the copyright of the thesis. I also retain the right to use in future works (such as articles or books) all or part of this thesis.

Erin Neely

April 9, 2020

Investigating Solvent Dynamics and Spin Probe Behavior Around the Intrinsically Disordered  
Protein  $\beta$ -Casein Through EPR Spectroscopy

by

Erin Neely

Kurt Warncke  
Adviser

Department of Physics

Kurt Warncke  
Adviser

Effrosyni Seitaridou  
Committee Member

David Lynn  
Committee Member

2021

Investigating Solvent Dynamics and Spin Probe Behavior Around the Intrinsically Disordered  
Protein  $\beta$ -Casein Through EPR Spectroscopy

By

Erin Neely

Dr. Kurt Warncke

Adviser

An abstract of  
a thesis submitted to the Faculty of Emory College of Arts and Sciences  
of Emory University in partial fulfillment  
of the requirements of the degree of  
Bachelor of Science with Honors

Department of Physics

2021

## Abstract

### Investigating Solvent Dynamics and Spin Probe Behavior Around the Intrinsically Disordered Protein $\beta$ -Casein Through EPR Spectroscopy

By Erin Neely

Intrinsically disordered proteins (IDPs)—those proteins that have no fixed, well-defined structure—and their dynamics within the cell are known to be important in human disease processes. Previously, globular proteins, such as ethanolamine ammonia-lyase (EAL) and myoglobin (Mb) have been studied by using electron paramagnetic resonance (EPR) spectroscopy, over the temperature range 195-265 K and at varying concentrations of dimethyl sulfoxide (DMSO) cosolvent. The paramagnetic nitroxide molecule, TEMPOL, which has EPR-detectable rotational motion—is used as a spin probe. Here, we report results for  $\beta$ -casein, representative of IDPs, over the temperature range 235-265 K and in the absence and presence of DMSO. EPR spectra were collected, and a Matlab algorithm was used to simulate the experiments and find the parameters (i.e., the weight and correlation times of both the fast and slow components of motion) of the best fit. Examination of temperature trends in the EPR spectra and numerical parameters reveals broad similarities in the EPR behavior of the globular and disordered proteins, but also—contrary to expectations—more rigid behavior continuing into higher temperature ranges in the  $\beta$ -casein system. Explanations of the protein and solvent dynamics responsible for the differing behavior are presented.

Investigating Solvent Dynamics and Spin Probe Behavior Around the Intrinsically Disordered  
Protein  $\beta$ -Casein Through EPR Spectroscopy

By

Erin Neely

Dr. Kurt Warncke

Adviser

A thesis submitted to the Faculty of Emory College of Arts and Sciences  
of Emory University in partial fulfillment  
of the requirements of the degree of  
Bachelor of Science with Honors

Department of Physics

2021

## Acknowledgements

First, I would like to acknowledge my advisor, Dr. Kurt Warncke. He agreed to take me on as an undergraduate researcher (when he did not have to do so) and supported me by finding a project that I could do and teaching me what I needed to know to do it. He also helped me revise and edit the project before submission.

Second, I would like to acknowledge the work of Wei Li and Katie Whitcomb, graduate students in Dr. Warncke's lab, for their help in putting this thesis together. Wei did the actual experimental work in person and sent me the data I would need. Both Wei and Katie helped me learn and practice the theory of EPR.

Third, I would like to acknowledge my parents, Chris and Michelle Neely, for supporting me as I worked to complete my thesis. Without their patience and their help with the technical aspects of Matlab and Microsoft Office, the road would have been a lot rockier.

Fourth, I would like to acknowledge Dr. David Lynn, endowed professor of chemistry, for agreeing to take the time out of his schedule to serve on my thesis defense committee and evaluate my project.

Last but not least, I would like to acknowledge Dr. Frosso Seitaridou, not only for also taking time out of her schedule to serve on my committee but for developing my love for physics and causing me to change my major. Without her, I never would have done this project at all.

## Table of Contents

I. Introduction	1
II. Experimental Procedures	7
a. Essential EPR	7
b. EPR Procedures	12
c. Automatic Simulations	13
d. Manual Adjustment	14
e. Data Analysis	15
III. Results and Discussion	16
a. The Spectral Patterns of Globular and Disordered Protein Systems are Highly Similar	23
b. The Use of 2% DMSO Cosolvent Creates More System Mobility	23
c. Correlation Times are Similar Between Systems of Globular and Disordered Proteins	24
d. The Intrinsically Disordered Systems Consistently Display A More Prominent Slow Component	24
IV. Conclusion	28
V. References	29

## List of Figures and Tables

### Figure

1	Diagram of $\beta$ -casein	2
2	Diagram of EAL experimental system	3
3	Myoglobin EPR spectra	5
4	Zeeman energy diagram	10
5	$\beta$ -casein EPR spectra	16
6	Component weights, 0% DMSO	18
7	Component weights, 2% DMSO	19
8	Component correlation times, 0% DMSO	21
9	Component correlation times, 2% DMSO	22

Table

1	Component weights, $\beta$ -casein	17
2	Logarithmic correlation times, $\beta$ -casein	20

## I. Introduction

The goal of this project is to use electron paramagnetic resonance (EPR) spectroscopy and computational EPR spectrum simulation techniques to study the behavior of intrinsically disordered proteins (IDPs), specifically  $\beta$ -casein. These proteins, defined by lacking a fixed structure in 3-space, are important objects of research, owing to the role that IDPs, such as  $\alpha$ -synuclein and p53 play in human diseases, ranging from cancer and diabetes to neurodegeneration and dementia (Uversky et al. 2008). IDPs have been studied before by using *nuclear* magnetic resonance or NMR (Adamski et al. 2019). The study of intrinsically disordered proteins by using EPR spectroscopy has been less prevalent.

$\beta$ -casein was chosen for study because it is representative of IDPs in general. There are technically many  $\beta$ -caseins, each being distinguished by specific variations in the amino acid structure. All  $\beta$ -caseins are phosphoproteins with 209 amino acid residues and molecular masses of approximately 24 kDa (Huppertz et al. 2018). Several prolines are distributed throughout the polypeptide chain (Eskin and Shahidi 2012), while the distribution of charged amino acids heavily favors the N-terminus (Huppertz et al. 2018). Throughout the protein chain, there are few  $\alpha$ -helices,  $\beta$ -sheets or disulfide bridges (see Figure 1), indicating lack of tertiary structure and intrinsic disorder.

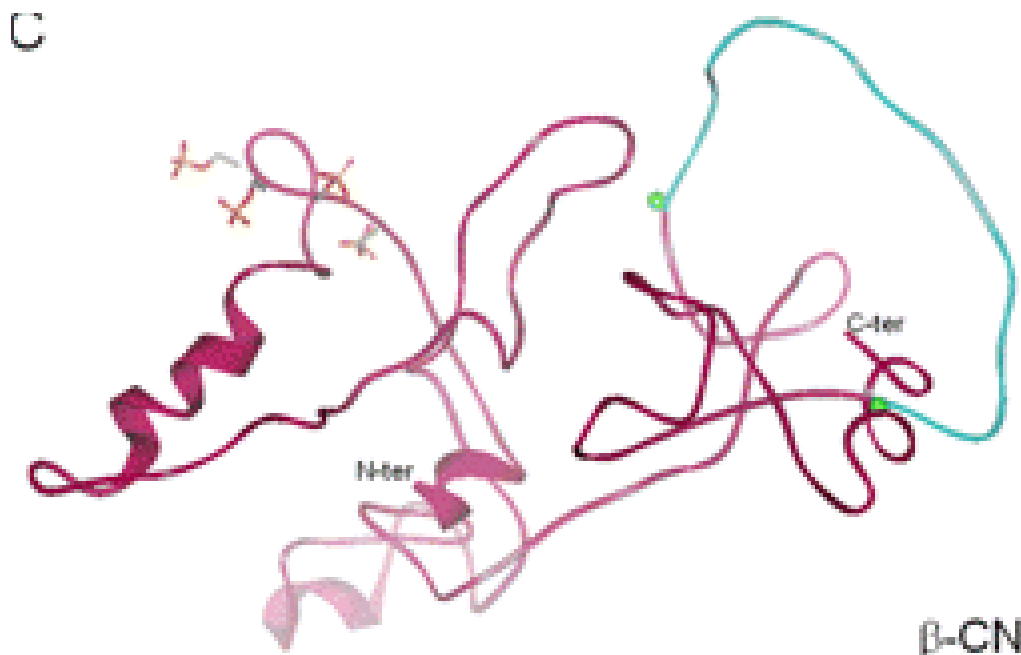


Figure 1: An illustration of the “structure” of  $\beta$ -casein. Coiled ribbons represent  $\alpha$ -helices; broad, flat ribbons represent  $\beta$ -sheets; orange crosses represent disulfide bridges. The blue region (surrounded by green spheres) represents hydrolysis in the source experiment, but the distinction is irrelevant for the purpose of this project. Image used with permission from Sadat-Mekmene et al. 2011.

EPR spectroscopy, as a technique, observes the transitions in the orientations (and therefore the energies) of electron dipoles in a magnetic field as microwave radiation is applied.<sup>1</sup> It is not applicable to studying  $\beta$ -casein (or most other proteins) directly, as  $\beta$ -casein lacks an unpaired electron which would give it a net magnetic dipole moment (Wertz and Bolton 1986).<sup>2</sup> However, EPR *can* be used to measure the electron spin transitions of the “spin probe” TEMPOL (a nitroxide radical), which when mixed into solution with the protein, will be informative about solution and protein behavior. Previous studies of globular proteins including myoglobin (Mb)

<sup>1</sup> EPR is actually very similar to the much more widely known technique of *nuclear magnetic resonance* (NMR), except that it takes advantage of the paramagnetic properties of electrons rather than the net spin of (certain) nuclei.

<sup>2</sup> Although electrons have paramagnetic properties from both their orbital and spin angular momenta, only the latter contribute significantly to the electron’s total magnetic dipole moment. Because the rules of electron interactions dictate that two electrons sharing the same orbital will always have opposite spins (and therefore opposite angular momenta), their magnetic dipole moments sum to zero and they do not have observable spin transitions.

and ethanolamine ammonia-lyase (EAL, shown in Figure 2) have demonstrated that when the solution into which the proteins are dissolved is frozen,<sup>3</sup> the expanding ice crystals “push” the spin probe into a small volume around the protein (Nforneh and Warncke 2019). This volume consists of two layers: the protein-associated domain, or PAD, and the mesodomain.

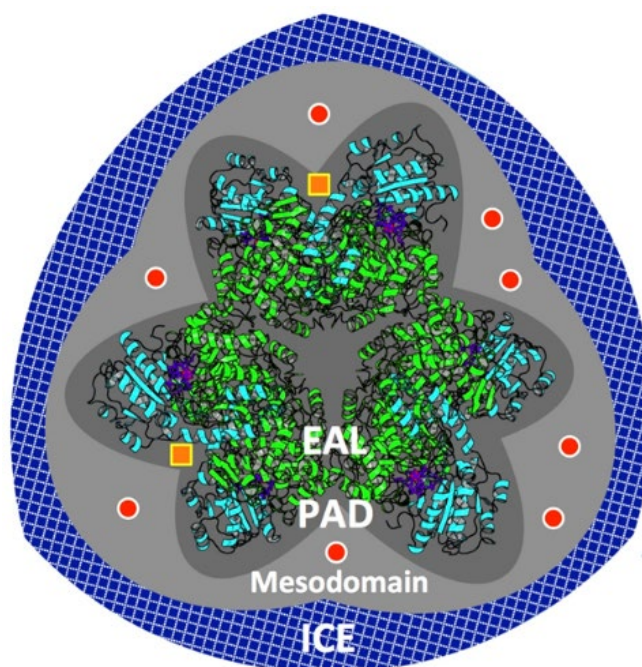


Figure 2: A diagram of the frozen aqueous solution of protein and spin probe used in previous EPR studies with ethanolamine ammonia-lyase, or EAL. Orange squares represent TEMPOL molecules in the protein-associated domain or PAD, and red circles represent TEMPOL molecules in the mesodomain. The dark gray layer is the PAD itself, while light gray represents the mesodomain.

The former is only observed in systems with protein and is thought to correspond to the protein’s hydration layer. The mesodomain is created when a cosolvent, such as dimethyl sulfoxide (DMSO) is added to the solution in relatively small proportion (here, 2% v/v), prior to freezing (Nforneh and Warncke 2019). TEMPOL has also been observed in previous experiments to rotate more rapidly (approximately 10-fold smaller rotational correlation time)

<sup>3</sup> EPR experiments only work at low (i.e., below freezing) temperatures anyway because at high temperatures, the electrons have large quantities of thermal energy that affects their behavior and prevents sufficient numbers of magnetic resonance transitions from being observed.

when it is localized in the mesodomain compared to the PAD (Nforneh and Warncke 2019). This allows conclusions to be drawn in the new  $\beta$ -casein experiments about the relative distribution and behavior of the spin probe in the PAD and mesodomain, as TEMPOL's rotational speed (analyzed through its proxy, the log of the correlation time or  $\log(\tau_{\text{corr}})$ ) has observable effects on the EPR spectra. When the rotation is slow and  $\log(\tau_{\text{corr}})$  is relatively large (approaching -7.0 to -6.0), the line shape is broadened, and the peaks are both wider and further apart.<sup>4</sup> When the rotation is fast and  $\log(\tau_{\text{corr}})$  is relatively small (approaching -10 to -11), the features are sharper, and the peaks are both narrower and closer together. These are the rigid and rapid rotation limits, respectively (Nforneh and Warncke 2019).

In addition to the location of the spin probe, temperature also has an appreciable effect on TEMPOL's motion because higher temperature, by definition, indicates more thermal motion. Higher temperatures should increase the rotational speed of both the "slow" component of the spin probe motions (in the PAD) and the "fast" component (in the mesodomain), and indeed this is what Nforneh and Warncke (2019) found. In their experiments with EAL, they observed an "order-disorder transition" (ODT) as the temperature increased, which corresponded to a spectral change from approaching the rigid limit to approaching the rapid limit. The same trend in EPR line shape dependence on temperature was observed for the globular protein, myoglobin, or Mb (Figure 3).

---

<sup>4</sup> There are three peaks on an EPR spectrum because there are three electron transitions, the electron Zeeman splitting being mediated by the hyperfine interaction with the nuclear spin (which can take one of three values).

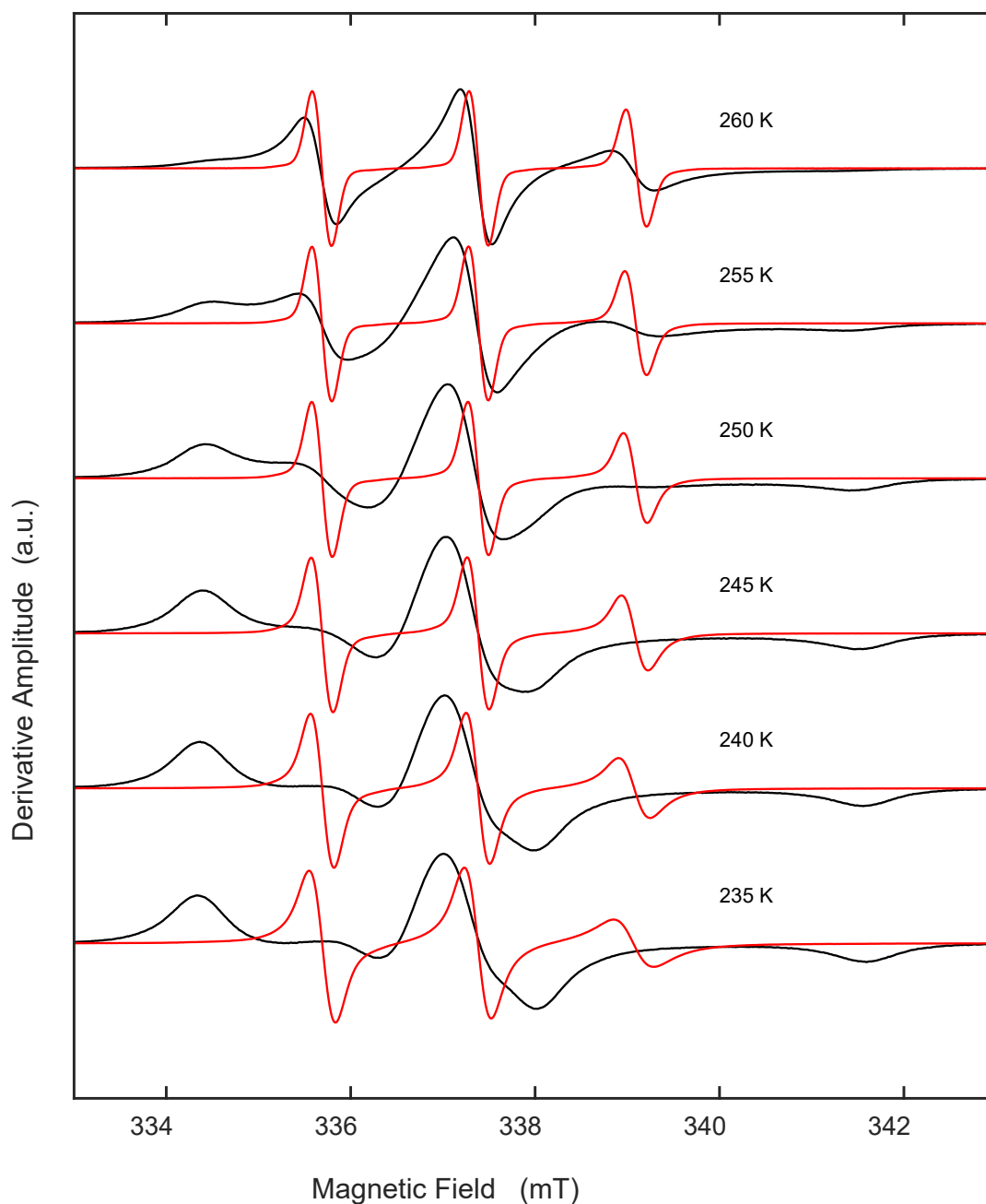


Figure 3: Example EPR spectra, taken for two systems of TEMPOL and the globular protein myoglobin in frozen polycrystalline aqueous solution. Black lines represent the system with no dimethyl sulfoxide (DMSO) cosolvent; red lines represent the system with 2% v/v DMSO added. For technical reasons including ease of observation of features, the instrument records the derivative of the absorption spectrum (with respect to the magnetic field  $B$ ) rather than the absorption spectrum itself. (Warncke, K., Li, W., unpublished)

As the temperature increases, the derivative peaks (appearing as hill-trough pairs) of energy absorption narrow and sharpen, indicating more rapid tumbling of the spin probe. For Mb, the specific order-disorder transition appears to occur at around 255 K (in the 0% DMSO experiment), where the low-field hill and high-field trough dramatically shrink in amplitude, and two more central hill-trough pairs start to appear.

Although  $\beta$ -casein is intrinsically disordered, similar behavior is expected: dividing the cryo-solution into a PAD with slow TEMPOL motion and a mesodomain with fast TEMPOL motion (and therefore the EPR spectrum into a slow and a fast component) and exhibiting an order-disorder transition over changing temperatures. The specifics of the spectral features and the numerical values that can be derived therefrom will be tested and may well be different, but the system should work in fundamentally the same way. Therefore, the same process that worked for the myoglobin experiments to discern TEMPOL's rotational motion should work for these new  $\beta$ -casein experiments. It is unfortunately not possible to discern the relative weights and correlation times of each spectral component directly from the overall spectrum, but it is possible to find them by using a computer to determine the values that lead to the best (optimized) match of a simulated EPR spectrum to the actual spectrum obtained by experiment. These optimized simulation parameters can be assumed to accurately reflect what is happening experimentally. Then, they can be compared to the corresponding values from the previous myoglobin experiments, in order to assess the differences in the solvent-protein interaction behavior between these representative cases of globular and disordered proteins.

## II. Experimental Procedures

### *Essential EPR*

EPR, essentially, examines the energy transitions owing to the absorption of microwave energy by electrons in a magnetic field. Because electrons are charged and have an angular momentum from both their orbit about the nucleus and their intrinsic spin, they have a magnetic dipole moment

$$\vec{\mu} = \frac{-1}{2} g_e \beta \hat{s} \quad (1).$$

$g_e$  is the electron  $g$ -factor,<sup>5</sup>  $\beta$  is the Bohr magneton, and  $\hat{s}$  is the unit vector in the direction of the electron's spin angular momentum. (Because the electron is negatively charged, the direction of its magnetic moment is reversed, compared to the direction of its spin.) Although electrons do have both an orbital and a spin angular momentum, the orbital contribution is so comparatively small for radicals that it is neglected here. When the electrons are placed in an external magnetic field  $\vec{B}$ , that field tends to align the dipoles along its axis, giving them an energy

$$E = -\vec{\mu} \cdot \vec{B} \quad (2).$$

Since the dot product is proportional to the magnitudes of both vectors and the cosine of the angle between them,  $E$  is at a maximum (most positive) when  $\vec{\mu}$  and  $\vec{B}$  are anti-parallel, and at a minimum (most negative) when they are parallel. However, because (due to the electron's negative charge)  $\vec{\mu}$  points opposite to the electron spin,  $\hat{s}$ ,  $E$  will be at a minimum when  $\hat{s}$  points against  $\vec{B}$ , and a maximum when  $\hat{s}$  points along  $\vec{B}$ . After substituting the appropriate values into

---

<sup>5</sup> This is actually a tensor but can be treated as a scalar in this case, since only one axis is considered.

the dot product, and defining spin “up” to be along  $\vec{B}$ , an electron in a magnetic field can have one of two equilibrium energies:<sup>6</sup>

$$E_{up} = +\frac{1}{2}g_e\beta B \quad (3)$$

or

$$E_{down} = -\frac{1}{2}g_e\beta B \quad (4).$$

The difference in these energies—and therefore the energy required for the electron dipole to transfer from spin down to spin up (or dipole down to dipole up)—is

$$\Delta E = g_e\beta B \quad (5).$$

In EPR, the energy used to flip the electron spins comes from an applied electromagnetic field. A photon has energy

$$E = h\nu, \quad (6)$$

where  $\nu$  is the frequency of the photon and  $h$  is Planck’s constant. Due to quantization of energy, the energy provided by the photon must exactly equal the energy required to flip the electron:

$$h\nu = g_e\beta B \quad (7).$$

This is called the *resonance condition*. When  $B$  is adjusted so as to meet this condition, the excess of electrons in the lower energy spin state absorb the energy of the photons, their spins flip, and the EPR spectrometer detects the absorption of energy. The EPR spectrum represents the derivative of the absorbance, because of the phase-sensitive detection scheme. This also

---

<sup>6</sup> Technically, the spin can have any orientation compared to the magnetic field. However, when the two vectors are not along the same line, the magnetic field exerts a torque on the electron dipole that aligns it along or against the field, so only those two orientations are considered.

makes the visual features in the EPR spectra easier to distinguish, and is why the peaks on the example spectra above (Fig. 3) are hill-valley pairs, not just hills.

The spectra in Fig. 3 also have *three* peaks each, rather than just one as the linear resonance condition would suggest, owing to the hyperfine (electron-nuclear) interactions of the electron dipoles with nuclear magnetic dipoles. There are two types of hyperfine coupling: the direct (isotropic, through-bond) and indirect (anisotropic, through-space) interactions. The isotropic hyperfine interactions arise from the nuclear spins present in TEMPOL that create nuclear magnetic dipoles: The most abundant isotope of oxygen,  $^{16}\text{O}$ , has nuclear spin quantum number  $I = 0$  (no hyperfine coupling), while  $^{14}\text{N}$  has nuclear spin quantum number  $I = 1$ . Together, then, the  $^{14}\text{N}$  have possible spin states  $m_I = -1, 0, \text{ and } +1$ . This multiplies with  $m_s$  and the hyperfine coupling constant  $A_{\text{iso}}$  to form an extra term in the Hamiltonian energy:

$$E_{\text{iso}} = m_s m_I * A_{\text{iso}} \quad (8).$$

Therefore, when  $\mu_s$  and  $\mu_I$  have the same sign, the energy of the electron increases; when they have opposite signs, the energy decreases. According to the selection rule, change of nuclear spin state is not allowed during an electron spin transition<sup>7</sup> Therefore, three total transition energies corresponding to each possible nuclear magnetic moment, result in three values of  $B$  (for a given  $\nu$ ) that create resonance, and correspondingly, three major features in the derivative spectra. These are shown in Figure 4.

---

<sup>7</sup> This is because, in the standard magnetic field range, the microwaves used to flip electron spins have too much energy to flip nuclear spins (which have a much lower Bohr magneton and a much lower transition energy).

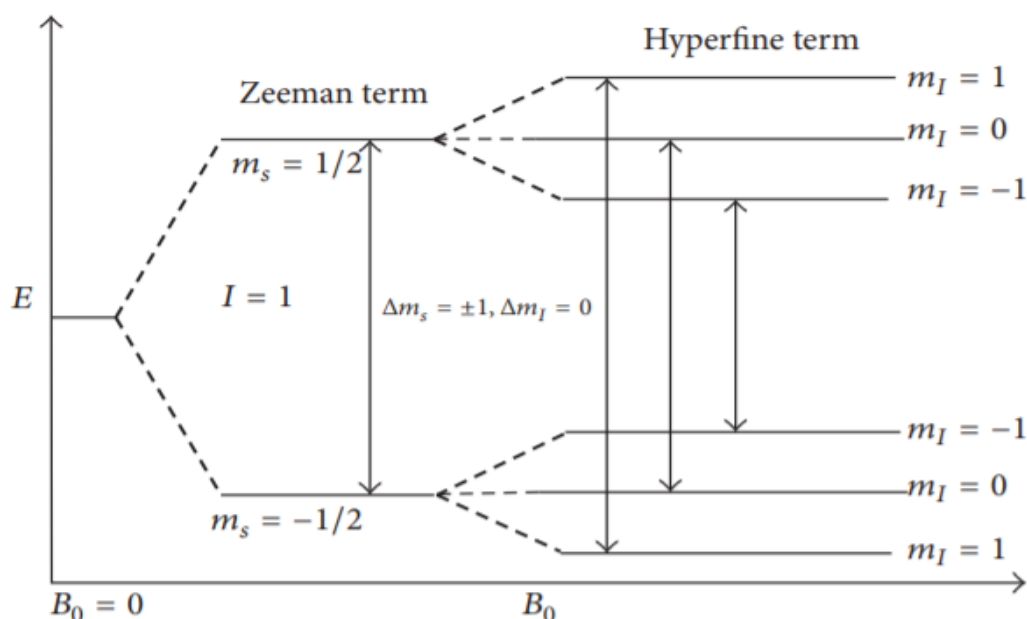


Figure 4: A diagram of the Zeeman energy splitting of coupled electron and nuclear spins. Used from Sahu and Lorigan, 2018 (under a Creative Commons license).

When  $m_I = +1$ , the energy level of  $m_s = -1/2$  decreases and the energy level of  $m_s = +1/2$  increases, leading to a larger energy split and therefore a lower value of  $B$  at resonance.<sup>8</sup> When  $m_s = -1/2$ , the reverse is true. Therefore, three derivative inflections are seen in the spectrum, corresponding to  $\mu_I = +1, 0$  and  $-1$  respectively. This direct hyperfine interaction is also called isotropic, because it does not depend on the orientation of the molecule itself relative to  $\vec{B}$ .

However, the indirect or anisotropic hyperfine interaction, which also affects EPR spectra, *does* depend on the orientation of the molecule: specifically, the  $z$ -component of the dipolar hyperfine interaction depends on the polar angle  $\theta$  between the electron spin and the radial vector from it to the nucleus (continuing to take the direction of  $\vec{B}$  as the  $+z$  direction and

<sup>8</sup> Since the difference between the energies of an electron's spin-up and spin-down orientations is proportional to  $B$ , using the same  $\nu$  (and therefore the same transition energy) while varying  $B$  requires a stronger magnetic field when the hyperfine coupling decreases the energy transition, and a weaker magnetic field when it increases the energy transition, in order to compensate for the hyperfine effects and achieve resonance.

assuming  $\vec{\mu}_s$  also points that way). This is because the magnetic field from a dipole is not uniform, but is stronger, closer to the poles. Therefore, the nuclear spin's interaction with the electron spin adds another term to the Hamiltonian:

$$E_{\text{an-iso}} = m_s m_I A_{\text{dip}} (3 \cos^2 \theta - 1) \quad (9)$$

where  $A_{\text{dip}}$  is the anisotropic coupling tensor, corresponding to the  $z$ -axis, or direction of the external magnetic field. The component in the  $xy$ -plane is not described, here. ( $A_{\text{dip}}$  being a tensor makes  $E_{\text{an-iso}}$  a tensor as well, but it is understood to refer to different changes in energy depending on the orientation of the nucleus relative to the electron spin). The effects of the direct and indirect hyperfine interactions combine to form the term

$$A = A_{\text{dip}} + A_{\text{iso}} \quad (10)$$

which appears in the simulation protocol.

The final complication of EPR—and the one that makes it so informative for the type of study reported here—is the effect of motion of the dipoles on EPR spectra. It was previously assumed, for the sake of explanation, that the only magnetic field aligning the electron dipoles was the external field  $\vec{B}$  in the  $+z$  direction, but that is not quite true: because microwave radiation is electromagnetic, it adds another magnetic field  $\vec{B}_1$  in the  $xy$ -plane that rotates with the microwaves' angular frequency  $\omega$  (Banerjee et al. 2009). As this approaches the dipoles' natural precession frequency

$$\omega_0 = \gamma B, \quad (11)$$

where  $\gamma$  is the gyromagnetic ratio, the electron's dipole moment  $\vec{\mu}_s$  aligns along

$$\vec{B}_{\text{eff}} = \vec{B} + \vec{B}_1 \quad (12).$$

Therefore, different polar angles  $\theta$  of the dipole (with respect to the  $+z$  axis) reflect different ratios of  $B_1$  to  $B$  (and correspondingly different  $\omega_0$ ) and have different transition energies. In a sample with several electron dipoles (such as the TEMPOL molecules used in the Warncke Lab's experiments), the dipoles start at different  $\theta$ , which broadens the spectral line, but their tumbling motion tends to average out the contributions of different  $\theta$  to the energy splitting and therefore the external field  $B$  required for resonance. The faster the TEMPOL rotation, the more averaging occurs, and the less the spectral features are broadened. This is reflected numerically in the parameter  $\log(\tau_{\text{corr}})$ , or the log of the correlation (i.e. rotation) time.

### *EPR Procedures*

The  $\beta$ -casein was prepared in solution with water, TEMPOL (In one sample) 2% v/v DMSO was also used. The samples were deep-frozen in liquid nitrogen-chilled isopentane at 140 K, and then placed in the EPR spectrometer and brought up through the temperature range 235-265 K. The applied microwave frequency was kept at a fixed value (approximately 9.5 GHz, but varying by  $\pm 0.005$  depending on the experiment) while the magnetic field was swept across a range of values between 332 and 346 mT. The spectrometer measured the derivative of the degree of radiation absorption with respect to the magnetic field strength and exported the results.<sup>9</sup>

---

<sup>9</sup> This is necessary for technical reasons: while for optical-spectrum collections an appropriate light emitter that can sweep a range of frequencies can be used, no such emitters exist for the microwave frequencies that are necessary in EPR, so the magnetic field  $B$  is swept across a range of values instead until the resonance condition is met and transitions occur.

### *Automatic Simulations*

Data from the spectrometer—the derivative of radiation absorption versus the magnetic field strength—from each experiment were converted to .mat workspace files and uploaded to the Matlab program. Then, scripts were written to simulate each experiment, using the `chili_2nuc` protocol. (“2nuc” means that the simulated spectrum will be a superposition of two spectra, one representing slow motion of the spin probe and the other representing fast motion.) In this protocol, Matlab accepts as input the various physical parameters of both the whole system (experimental microwave frequency, experimental temperature, array of magnetic field values used) and of each spectral component (the g-tensor, the A-tensor, its relative weight, its line width, and the log of its correlation time.) Then, it varies over a user-specified interval (the “Vary values”) the parameters of both the “slow” and “fast” simulation component. When it finds which values produce a simulated spectrum closest to the experimental result (i.e., minimize the error), it plots the simulated spectrum over the experimental spectrum and returns the optimized values.

In order to begin the simulation process, optimized component parameters were copied over from a previously completed myoglobin simulation at 265 K and 0% DMSO into the script for the corresponding (i.e., 265 K and 0% DMSO) beta-casein simulation. A value for the microwave frequency was copied over from the “FrequencyMon” entry in the parameters file attached to the workspace. All Vary values were set to 0, save for the line width of the fast component (which was set to a “dummy” value on the order of  $10^{-6}$  so that the simulation would execute). The simulation was executed several times, with the microwave frequency value being manually adjusted each time (first by megahertz, then by tenths of megahertz) until the central points of inflection of the simulated and experimental spectra were “lined up” horizontally as

closely as possible. Alignment was checked first visually, then numerically (by examining—and seeking to minimize—the value of the rmsd curve-fit-error parameter returned by the program). This process ensured that horizontal misalignment caused by errors in the microwave frequency value used by the program would not interfere with proper curve fitting in the actual simulation.

With the microwave frequency optimized, all starting values of the component parameters were rounded to one decimal place. Then, all Vary values were made non-trivial, being set to anywhere between 0.3 and 1.0 depending on the expected drift of the corresponding parameter from its starting value. However, they were always set so that no optimized parameter (which would always be in the range of the starting parameter +/- its Vary value) could ever be negative, and the line widths were not permitted to exceed 0.8. The simulation was executed, returning a figure and six optimized parameters—the weight, line width, and  $\log(\tau_{\text{corr}})$  for components A and B. The numbers were copied to an Excel spreadsheet and the figure was saved. This procedure was repeated for temperatures down to 235 K by increments of 5 K, with the starting parameters each time being the optimized parameters from the last simulation. The simulations for the systems with 2% DMSO added followed the same procedures.

### *Manual Adjustment*

Because the chili\_2nuc simulation protocol finds the best fit for the experimental spectrum as a whole and therefore may not accurately fit the trends in certain specific areas, it was necessary to manually adjust the  $\log(\tau_{\text{corr}})$  of the slow component in order to fit the low-field “wing” appearing immediately before the first point of inflection of the 2% DMSO spectra taken at 245, 250, and 255 K. (See Figure 5.) For each of these spectra, the code for the automatic simulations was copied and pasted seven times, forming distinct sections labelled  $n=0$  through

$n=6$ . All parameters for the system as a whole were copied over from the corresponding parameters used in the fully automatic simulations (including the optimized microwave frequency), and all starting values of the component parameters were set to their optimized values from the fully automatic simulations. All “Vary” values were set to 0, save for a “dummy” value of the line width of the fast component on the order of  $10^{-6}$  (so that the simulation would run). For convenience, the magnetic field array, the system parameters and the component parameters (both their starting and variation values) were cut from the sections and moved to the front of the code. Then, in each section, Sys1.logtcorr, the  $\log(\tau_{\text{corr}})$  of the slow component, had  $0.1n$  added to it. This was based on how much manual correction was necessary in previous experiments. The entire code was run, displaying a separate figure at the end for each value of  $n$ . Each figure was analyzed visually, to determine the value of  $n$  that offered the best balance of fit between the low-field wing and the rest of the spectrum.

### *Data Analysis*

After each automatic simulation, experimental data were recorded in an Excel spreadsheet. The weights of the slow and fast component for each simulation were normalized (divided by their sum) to more clearly reflect the proportion of slow- and fast-moving spin probes. The normalized weights and  $\log(\tau_{\text{corr}})$  values were sorted by data type and the presence or absence of DMSO in order to form separate row arrays across the range of temperatures, 235-265 K. The equivalent data for previous experiments with EAL were copied from the Nforneh and Warncke papers (0% data from 2017, 2% data from 2019) into other row arrays. These row arrays were inserted into Matlab and used to graph Figures 6–9 under “Results.”

### III. Results and Discussion

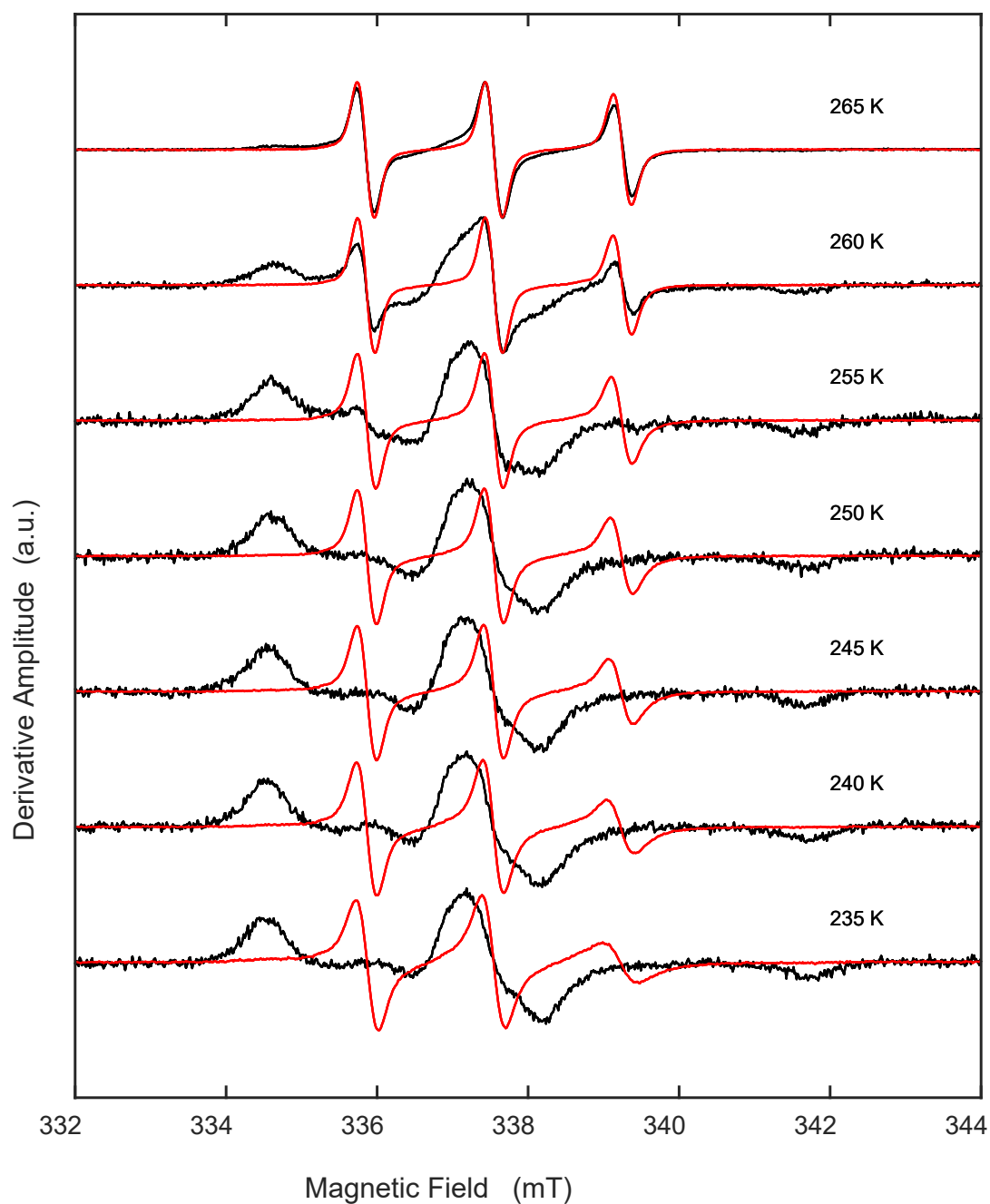


Figure 5: The experimental EPR spectra of the  $\beta$ -casein system, taken over temperatures increasing from 235 to 265 K in 5K increments. The black line represents the sample with no DMSO added, and the red line represents the sample with 2% v/v DMSO added. As the temperature increases, the derivative features narrow and sharpen, for both the 0% and 2% DMSO spectra. At every temperature, however, the 2% DMSO spectra

Table 1: The relative weights of the slow and fast components of the EPR spectra collected in the current experiments with  $\beta$ -casein. Numbers have been rounded to four decimal places.

Temperature (Kelvin)	0% DMSO		2% DMSO	
	Slow	Fast	Slow	Fast
235	0.1028	0.8972	0.4848	0.5152
240	0.1169	0.8831	0.4639	0.5361
245	0.1231	0.8769	0.4522	0.5478
250	0.7903	0.2097	0.4550	0.5450
255	0.7350	0.2650	0.4458	0.5542
260	0.9184	0.0816	0.3933	0.6067
265	0.6965	0.3035	0.3842	0.6158

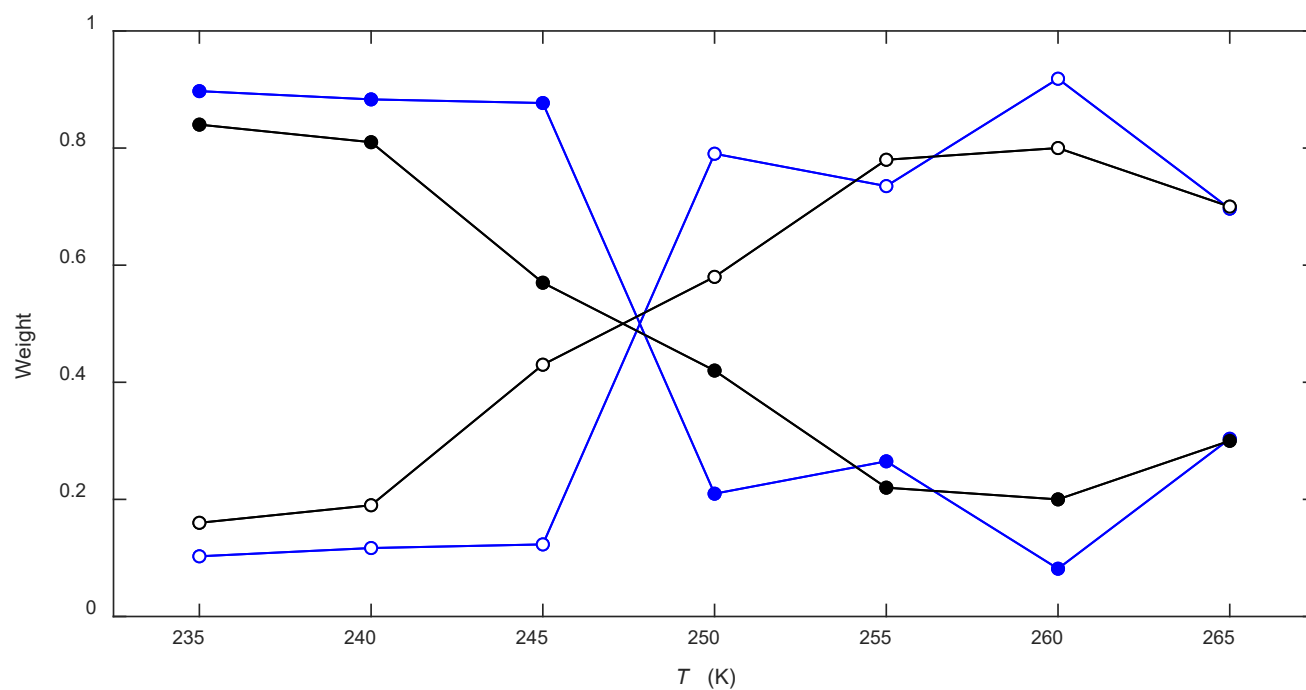


Figure 6: The relative normalized weights of each component of both the  $\beta$ -casein (blue line) and EAL (black line) systems with 0% DMSO. Slow components are represented by open circles; fast components are represented by closed circles. At low temperature, fast components appear to be dominant; at high temperature, the values “switch” and slow components become dominant, for both protein systems.

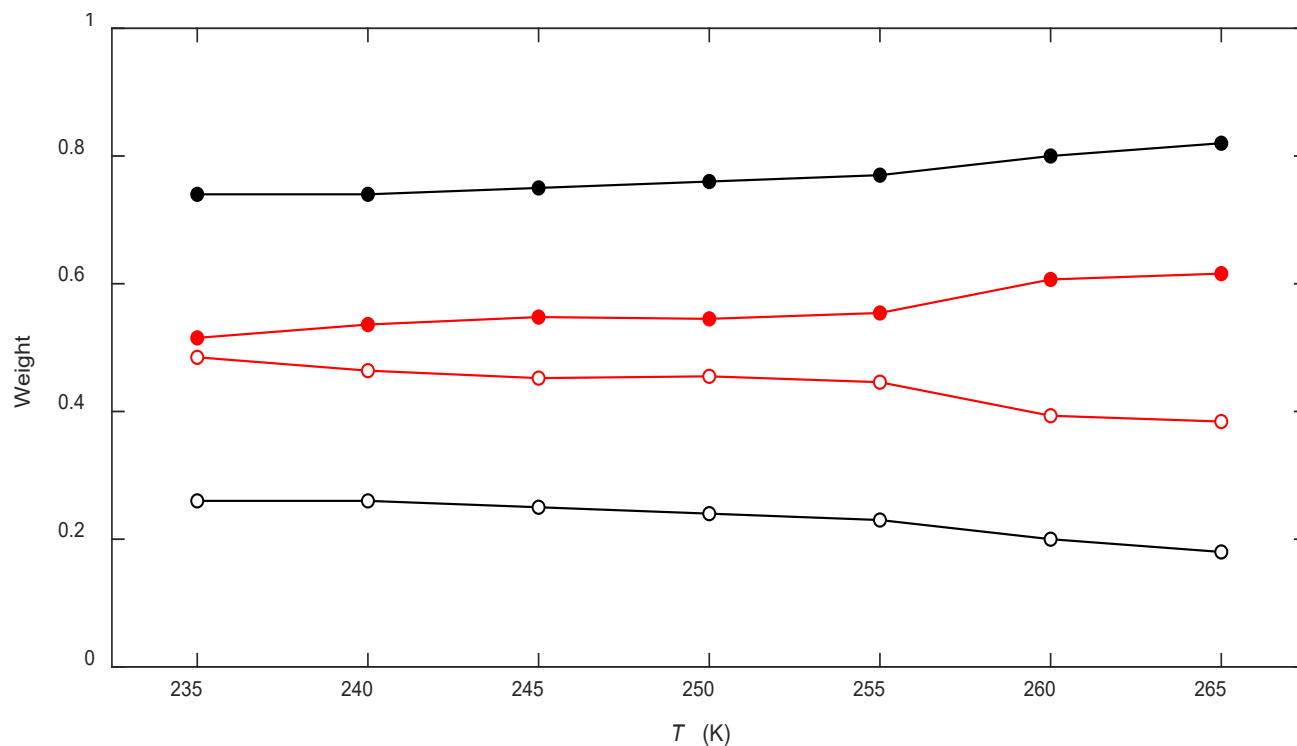


Figure 7: The relative normalized weights of each component of both the  $\beta$ -casein (red line) and EAL (black line) systems with 2% DMSO. Slow components are represented by open circles; fast components are represented by closed circles. For both proteins, fast components slightly increase in weight as the temperature rises; however, at all temperatures,  $\beta$ -casein displays a significantly more prominent slow component.

Table 2: The relative logarithmic correlation times of the slow and fast components of the EPR spectra collected in the current experiments with  $\beta$ -casein. Numbers have been rounded to two decimal places.

Temperature (Kelvin)	0% DMSO		2% DMSO	
	Slow	Fast	Slow	Fast
235	-6.39	-7.10	-8.49	-9.02
240	-6.71	-7.29	-8.70	-9.18
245	-6.54	-7.45	-8.91	-9.32
250	-7.26	-8.36	-9.09	-9.45
255	-7.40	-8.58	-9.25	-9.58
260	-7.91	-9.43	-9.36	-9.79
265	-8.43	-9.76	-9.64	-9.97

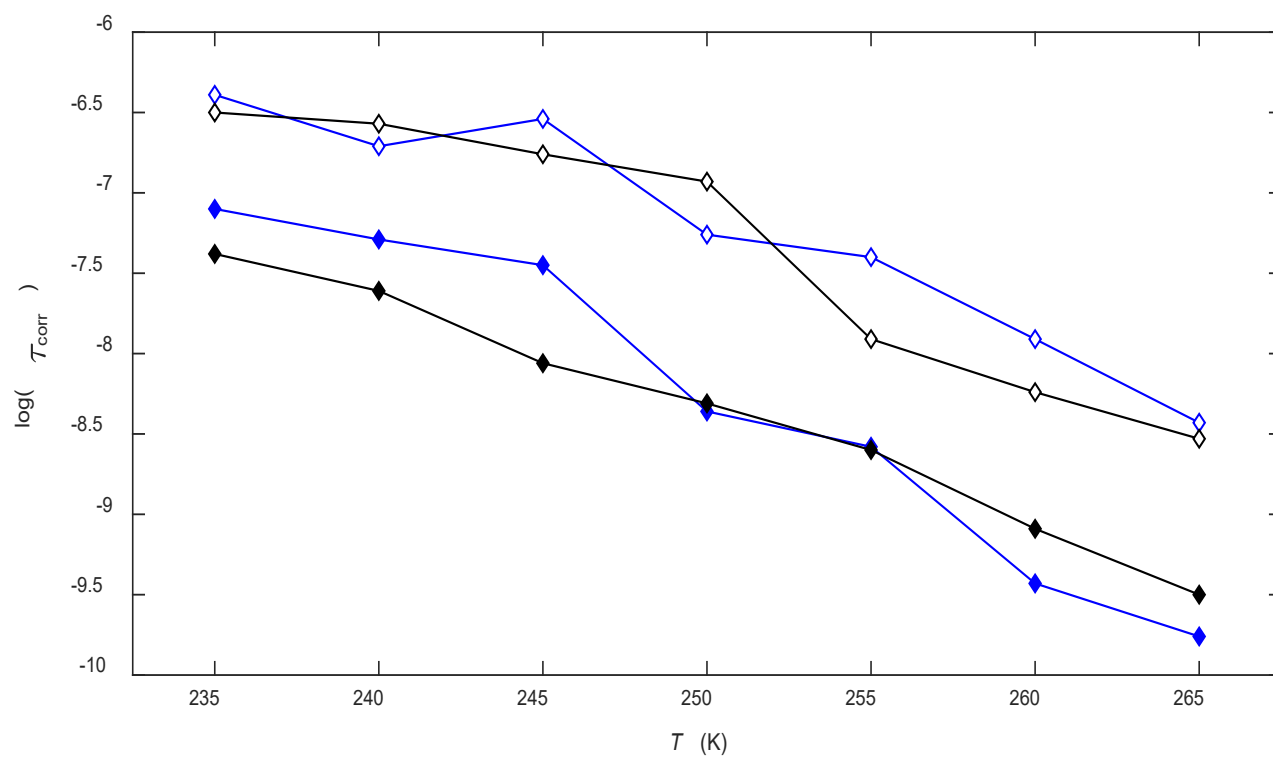


Figure 8: The logarithmic correlation times of each component of both the  $\beta$ -casein (blue line) and EAL (black line) systems with 0% DMSO. Slow components are represented by open diamonds; fast components are represented by closed diamonds. In each system, the fast component has a more negative  $\log(\tau_{\text{corr}})$  and a faster correlation time. As the temperature increases, differences in  $\log(\tau_{\text{corr}})$  of the slow component between the two protein systems are not consistent.

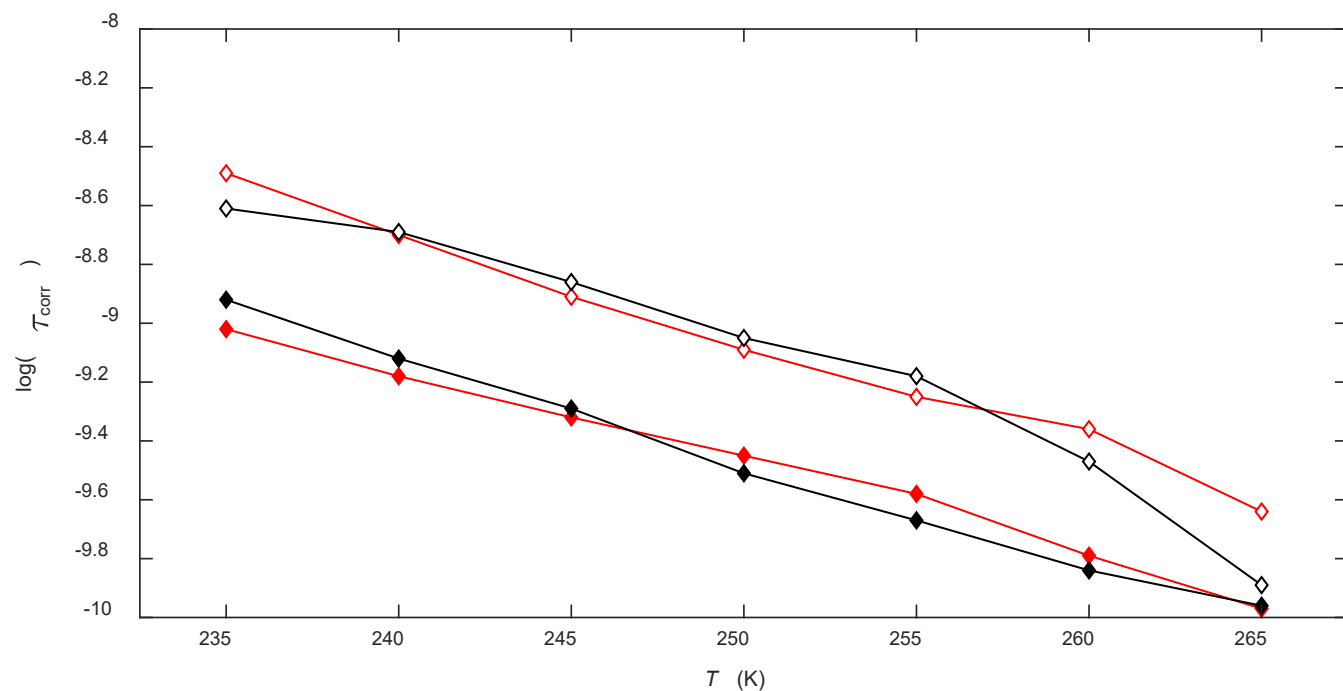


Figure 9: The logarithmic correlation times of each component of both the  $\beta$ -casein (red line) and EAL (black line) systems with 2% DMSO. Slow components are represented by open diamonds; fast components are represented by closed diamonds. In each system, the fast component has a more negative  $\log(\tau_{\text{corr}})$  and a faster correlation time. As the temperature increases, differences in  $\log(\tau_{\text{corr}})$  of the slow component between the two protein systems are very minor.

### *The Spectral Patterns of Globular and Disordered Protein Systems are Highly Similar*

Figures 3 and 5, the corresponding EPR spectra for myoglobin and  $\beta$ -casein show, fundamentally, the same behavior. The derivative amplitude shows three main features, with significant line broadening at lower temperatures. In the experiments without DMSO, the  $\beta$ -casein spectra—like the myoglobin spectra—show a low-field peak and a high-field trough that slowly shrink in amplitude and turn into additional mid-field peak-trough pairs as the temperatures increases. This marks the order-disorder transition. Similarly, in the experiments with DMSO, both sets of spectra show less line broadening (than the 0% spectra) and three distinct peak-trough pairs that get narrower and sharper as  $T$  increases. Furthermore, after the microwave frequency correction, both sets of spectra are aligned horizontally (i.e., their relevant features occur at the same values of  $B$ ). Since the temperature-dependence of the Mb and EAL EPR spectra are essentially identical (Nforneh and Warncke, 2017, 2019; Warncke, K., Li, W., unpublished), their simulation data, which are derived from the EPR spectra, can also be assumed to lack any significant differences. Therefore, the direct EPR spectra from the Mb experiments and the simulation data from the EAL experiments are used together as a point of comparison for the behavior of  $\beta$ -casein.

### *The Use of 2% DMSO Cosolvent Creates More System Mobility*

At every temperature studied, the spectra collected for both myoglobin and  $\beta$ -casein with 2% v/v DMSO are smoother and show sharper features, in accord (for both EAL and  $\beta$ -casein) with  $\log(\tau_{\text{corr}})$  being more negative for both the fast and slow components and the weight of the fast component being higher in the 2% DMSO system at high  $T$ . Nforneh and Warncke (2019) also observed this in their experiments with EAL, and theorized that added DMSO increases the

volume of the mesodomain, which allows more spin probes to move into the mesodomain where they are less confined by the protein and can rotate faster. This was observed in previous studies of globular proteins, and the observation is confirmed by the present study of  $\beta$ -casein.

#### *Correlation Times are Similar Between Systems of Globular and Disordered Proteins*

After examining Figures 8 and 9, there are differences in the  $\log(\tau_{\text{corr}})$  values between the EAL and  $\beta$ -casein systems, when holding temperatures and DMSO concentrations constant. However, these differences are relatively minor (never exceeding 0.3), and the two sets of lines repeatedly intersect each other. One trial is reflected in the  $\beta$ -casein data, so these differences may not be significant. Further testing, with multiple samples and possibly more refined simulation procedures, is needed to examine these differences and determine how significant they are. But assuming that the correlation times of both protein systems are in fact broadly similar when holding other conditions constant, this suggests that the PAD and mesodomain respectively around each protein are broadly similar environments, creating similar rotational dynamics for the spin probes within them. Both the surface topography of EAL and the open structure of  $\beta$ -casein may create solvent microenvironments that surround spin probes and shape their motion.

#### *The Intrinsically Disordered Systems Consistently Display A More Prominent Slow Component*

However, there are some differences between the behavior of  $\beta$ -casein versus globular proteins. In the systems without DMSO (see Figures 3 and 5), the  $\beta$ -casein spectra consistently “lag” the Mb spectra by about 5 K. That is, if an Mb spectrum behaves a certain way at

temperature  $T$ , the  $\beta$ -casein spectrum at  $(T+5)$  K will behave in a similar way. The features of the  $\beta$ -casein spectra indicating a prominent slow component of spin probe motion—the low-field peak and high-field trough—are sharper, larger in amplitude, and persist to higher temperatures compared to those of the Mb spectra. Between  $T = 255$  K and  $T = 260$  K in particular, the Mb spectrum shifts in ways (namely, the narrowing and sharpening of the derivative features) that the  $\beta$ -casein spectrum does not. Therefore, if the order-disorder transition can be tied to a specific temperature point, that point is about 5 K higher for  $\beta$ -casein than it is for myoglobin.

In the experiments with 2% DMSO cosolvent, the behavior of the two sets of spectra (in Figures 3 and 5) is even more similar than it is with 0% DMSO under visual inspection. There is still one key difference, however: at all temperatures, the  $\beta$ -casein spectra show traces of a slow component. It is very difficult to see visually, but at high values of  $T$ , the  $\beta$ -casein spectra show traces of line broadening that the Mb spectra lack. Additionally, at low values of  $T$ , the  $\beta$ -casein spectra show a small positive slope at low field, indicating a component approaching the rigid limit. This is consistent with the observation from Figure 7 that at every temperature, the slow component has a higher weight in the  $\beta$ -casein system than in the EAL system. Figure 9 (the correlation time plot for the 2% DMSO experiments) does show that the  $\beta$ -casein system is not approaching the rigid limit, even at 235 K: the value of  $\log(\tau_{\text{corr}})$  is too negative. However, the simulation algorithm only fits two components of motion, so it could be misleading, if in physical reality the system has three components (a fast, a slow, and a very slow). This is certainly possible, given the intrinsically disordered nature of  $\beta$ -casein: surface irregularities could “trap” some spin probes to be even more associated with the protein.

Furthermore, it is probable—given the consistent higher weight of the slow component for the  $\beta$ -casein systems (at 2% DMSO, Figure 7) compared to the Mb and EAL systems—that

the volume of the PAD is expanded relative to that of the mesodomain around an intrinsically disordered protein. This confirms our prediction, which was based on the fact that since IDPs are unstructured, they are likely to have larger surface areas given the same volume. However, the data contradict our prediction that due to the very same intrinsically disordered nature of  $\beta$ -casein, its spectra would show more mobility at lower temperatures than those of globular proteins. The latter prediction was based on the hypothesis of solvent microenvironments created by structural gaps, which would activate motion. However, the globular protein EAL also has an uneven surface topography, including “water network breaking regions”. So solvent microenvironments may have the same or greater effects around globular proteins. It is also possible that the folded-up globular protein, unlike the disordered extended protein chain, may be able to move as a unit and carry the spin probes with it, adding to their motion. This hypothesis could possibly be tested by labeling the proteins themselves with something sensitive to EPR and/or NMR, such as  $^{13}\text{C}$  or  $^{15}\text{N}$  (Clare and Gronenborn 1991).

Another possible explanation for the decrease in mobility in the intrinsically disordered system is condensation and phase-separation of the IDP. This is known to happen in biological systems, including with proteins (Leslie 2021). If this is the case, it may trap TEMPOL and interfere with its EPR signal; in fact, this is suggested by the observed poor signal-to-noise ratio in the  $\beta$ -casein experiments compared to those with globular proteins. (Figure 5, unlike Figure 3, shows a decrease in signal-to-noise ratio in the 0% DMSO spectra,) Further testing is needed to examine any possible phase separation in  $\beta$ -casein and other IDPs in the low-temperature, frozen solution system, such as by fluorescence microscopy or 1, 6-hexanediol application (Leslie 2021). However, regardless of whether this hypothesis is true or not, there is clearly still some

signal from the  $\beta$ -casein systems, so it is likely that a significant proportion of spin probes remain unaffected, and our other hypotheses are not ruled out.

## IV. Conclusion

In summary, the behavior of the intrinsically disordered protein  $\beta$ -casein in EPR experiments with the spin probe TEMPOL shows both significant differences and significant similarities to that of the globular proteins myoglobin and EAL. The two sets of EPR spectra display a broadly similar pattern (between temperatures and DMSO concentrations), and the use of 2% DMSO cosolvent has similar motion-increasing effects. However, contrary to our expectations, the behavior of the spin probes surrounding  $\beta$ -casein showed more rigidity and a temperature lag of about 5 K compared to those surrounding globular proteins. This could be due to any combination of increased confinement effects of the protein chain, lack of uniform protein motion, and phase separation, all of which can be illuminated by further testing. Although the conditions of EPR obviously differ greatly from *in vivo* conditions, this research and its follow-up studies can still be applicable to critical biomedical research, because IDPs are known to be involved in human diseases and examining both their own tendencies and the behavior of solvents and spin probes around them may reveal those mechanisms and offer clues for therapies. This study may represent the beginning of EPR examination of intrinsically disordered proteins, but it is by no means the end.

## V. References

- Adamski, W., Salvi, N., Maurin, D., Magnat, J., Milles, S., Jensen, M. R., ... & Blackledge, M. (2019). A unified description of intrinsically disordered protein dynamics under physiological conditions using NMR spectroscopy. *Journal of the American Chemical Society*, *141*(44), 17817-17829.
- Banerjee, D., Bhat, S. N., Bhat, S. V., & Leporini, D. (2009). ESR evidence for 2 coexisting liquid phases in deeply supercooled bulk water. *Proceedings of the National Academy of Sciences*, *106*(28), 11448-11453.
- Clore, G. M., & Gronenborn, A. M. (1991). Applications of three-and four-dimensional heteronuclear NMR spectroscopy to protein structure determination. *Progress in nuclear magnetic resonance spectroscopy*, *23*(1), 43-92.
- Eskin, N. M., & Shahidi, F. (2013). *Biochemistry of foods*. Amsterdam, Netherlands: Elsevier/Academic Press. doi:10.1016/C2009-0-02724-X
- Leslie, M. (2021). Separation anxiety. *Science*. doi:10.1126/science.371.6527.336.
- Nforneh, B., & Warncke, K. (2017). Mesodomain and protein-associated solvent phases with temperature-tunable (200–265 K) dynamics surround ethanolamine ammonia-lyase in globally polycrystalline aqueous solution containing dimethyl sulfoxide. *The Journal of Physical Chemistry B*, *121*(49), 11109-11118.
- Nforneh, B., & Warncke, K. (2019). Control of Solvent Dynamics around the B12-Dependent Ethanolamine Ammonia-Lyase Enzyme in Frozen Aqueous Solution by Using Dimethyl Sulfoxide Modulation of Mesodomain Volume. *The Journal of Physical Chemistry B*, *123*(26), 5395-5404.
- Sadat-Mekmene, L., Jardin, J., Corre, C., Mollé, D., Richoux, R., Delage, M. M., ... & Gagnaire, V. (2011). Simultaneous presence of PrtH and PrtH2 proteinases in *Lactobacillus*

- helveticus strains improves breakdown of the pure  $\alpha$ s1-casein. *Applied and environmental microbiology*, 77(1), 179-186.
- Sahu, I. D., & Lorigan, G. A. (2018). Site-directed spin labeling EPR for studying membrane proteins. *BioMed research international*, 2018.
- Uversky, V. N., Oldfield, C. J., & Dunker, A. K. (2008). Intrinsically disordered proteins in human diseases: introducing the D2 concept. *Annu. Rev. Biophys.*, 37, 215-246.
- Wertz, J. E., & Bolton, J. R. (1986). Biological Applications of Electron Spin Resonance. In *Electron Spin Resonance* (pp. 378-390). Springer, Dordrecht.